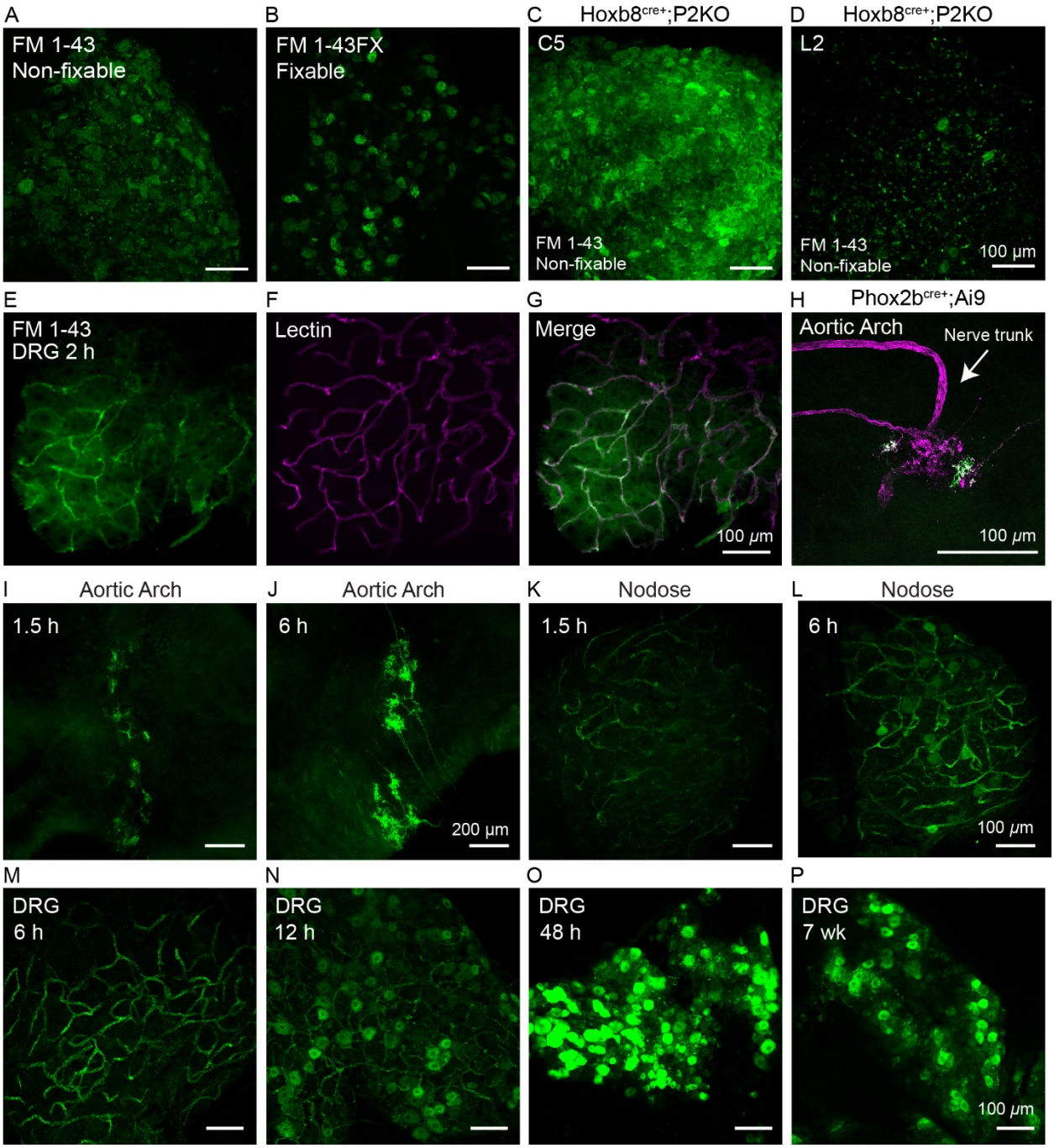


**<u>Figure S1</u>: Patterns and timing of FM 1-43 labeling, related to Figure 1**

(A–B) FM 1-43 (non-fixable) and FM 1-43FX (fixable) fluorescent signal in lumbar DRG, 24 h post i.p. dye injection.

(C–D) FM 1-43 (non-fixable) labeling in a C5 cervical and L2 lumbar DRG from Hoxb8$^{cre+}$;P2KO mouse 24 h post i.p. non-fixable FM 1-43 injection.

(E) Z-stack of lumbar DRG 2 h post i.p. FM 1-43 injection showing FM 1-43 labeling pattern.

(F) Perfusion-based tomato lectin (DyLight 649) staining of the same DRG marking vasculature within DRG.

(G) Merged image showing overlap between FM 1-43 signal and lectin. Scale bar applies to E-G.

(H) Z-stack image of example aorta baroreceptor endings from a Phox2b$^{Cre+}$;Ai9 mouse injected i.p. with FM 1-43 24 h prior to tissue collection. Tdtomato (magenta) and FM 1-43 (green) channels are displayed as a single merged image. Green endings are also tdTomato+, but some tdTomato+ endings did not label with FM 1-43.

(I–J) Representative FM 1-43 labeling pattern in the aorta baroreceptor endings after 1.5 h (I), and 6 h (J) of FM 1-43 labeling. Scale applies to both.

(K–L) Representative FM 1-43 labeling in the nodose ganglion after 1.5 h (K) and 6 h (L) of FM 1-43 labeling. Same animal from panels (I) and (J) respectively. Scale applies to both.

(M–P) Representative z-stack of whole-mount lumbar DRG from wildtype mice injected i.p. with FM 1-43 6 h (M), 12 h (N), 48 h (O), and 7 weeks (P) before tissue collection. Scale bar applies to M-P.

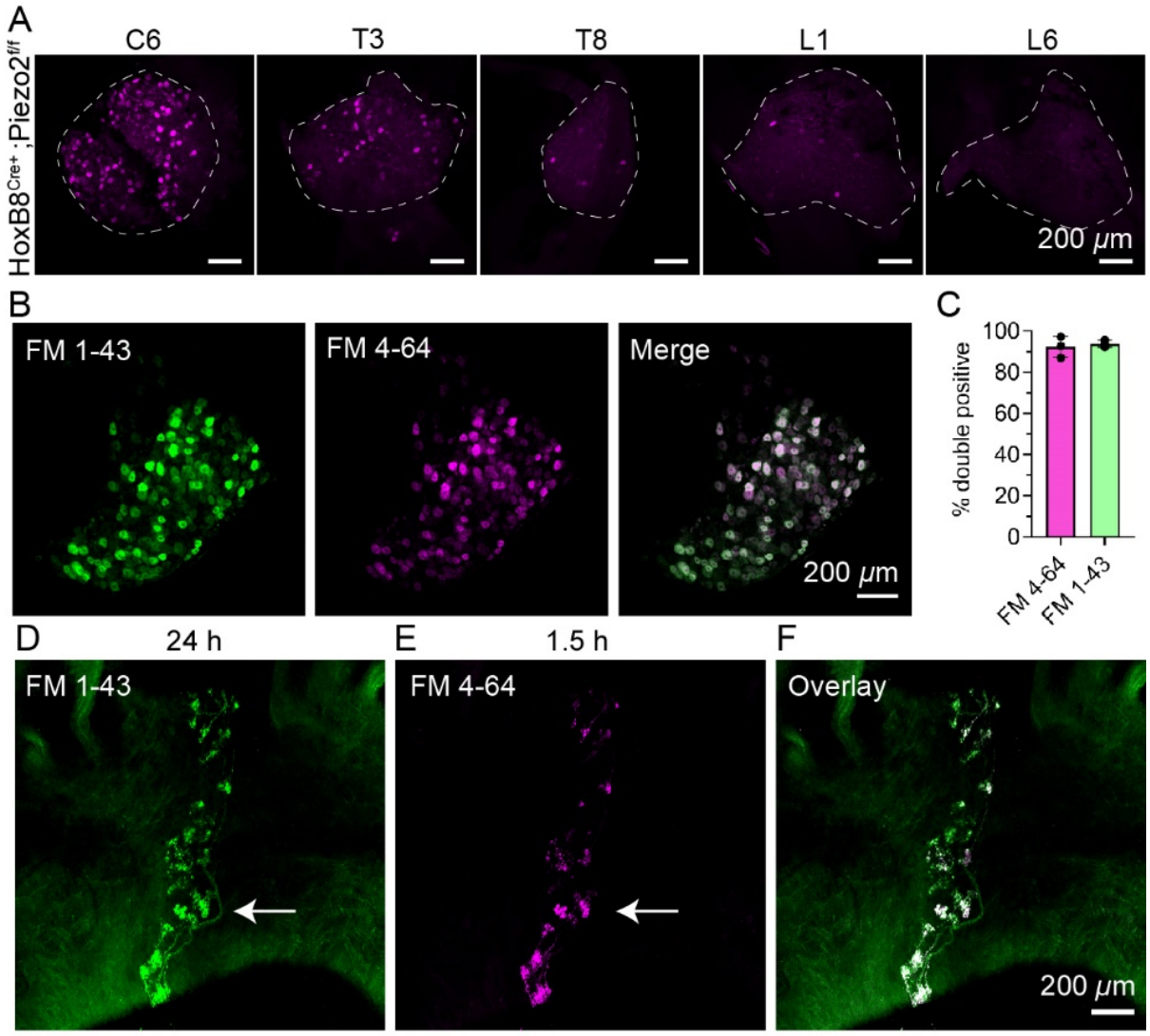


**Figure S2: FM 4-64 sensory neuron labeling pattern is consistent with FM 1-43, related to Figure 1**

(A) Representative z-stack images of whole-mount DRGs from *HoxB8$^{Cre+}$;Piezo2$^{f/f}$* male mouse injected with FM 4-64 24 h prior. The DRG level is indicated. Scale bar applies to all images.

(B) DRG from a wildtype mouse injected i.p. with both FM 1-43 (green) and FM 4-64 (magenta) 24 h prior to tissue harvest. Merged image shown on right. Scale bar applies to all images.

(C) Quantification of FM 1-43 and FM 4-64 'Double Positive' cell bodies expressed as a percent. Dots represent individual DRGs from a single male mouse, data shown with mean ± SD.

(D) FM 1-43 labeling in a whole-mount aorta from an animal injected with FM 1-43 24 h before tissue harvest. Arrow points to nerve trunk. Scale bar applies to D–F.

(E) The same baroreceptor endings in D, labeled by FM 4-64 injected 1.5 h before tissue harvest.

(F) Merge of D and E. White represents areas of overlap.

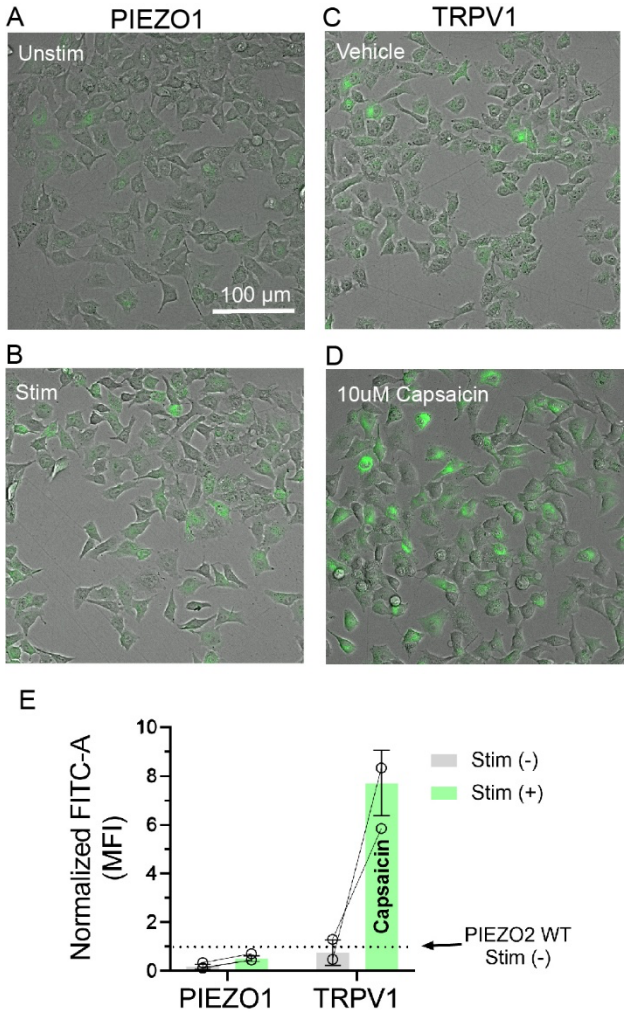


**Figure S3: TRPV1 and PIEZO1 overexpression induces FM 1-43 uptake in cell culture, related to Figures 4 and 5**

(A) Representative image from HEKP1 KO cells transfected with human PIEZO1 treated with 10 µM FM 1-43 without shaking ('Unstim'),

(B) and with exposure to orbital shaking ('Stim').

(C) Representative image from HEKP1 KO cells transfected with rat TRPV1 treated with 10 µM FM 1-43 and vehicle control (EtOH),

(D) and 10 µM FM 1-43 and 10 µM capsaicin.

(E) Flow cytometry quantification of each condition background subtracted and expressed relative to the levels observed in unstimulated HEK P1KO cells transfected with hPIEZO2 WT (shown as a dotted line). Individual symbols represent biological replicates, data shown as mean ± SD. (Piezo1, p=0.0013, Unpaired two-tailed t test, N=3 experimental replicates and TRPV1, N=2 experimental replicates, represented by circles). Connecting lines represent experiments run on the same day.

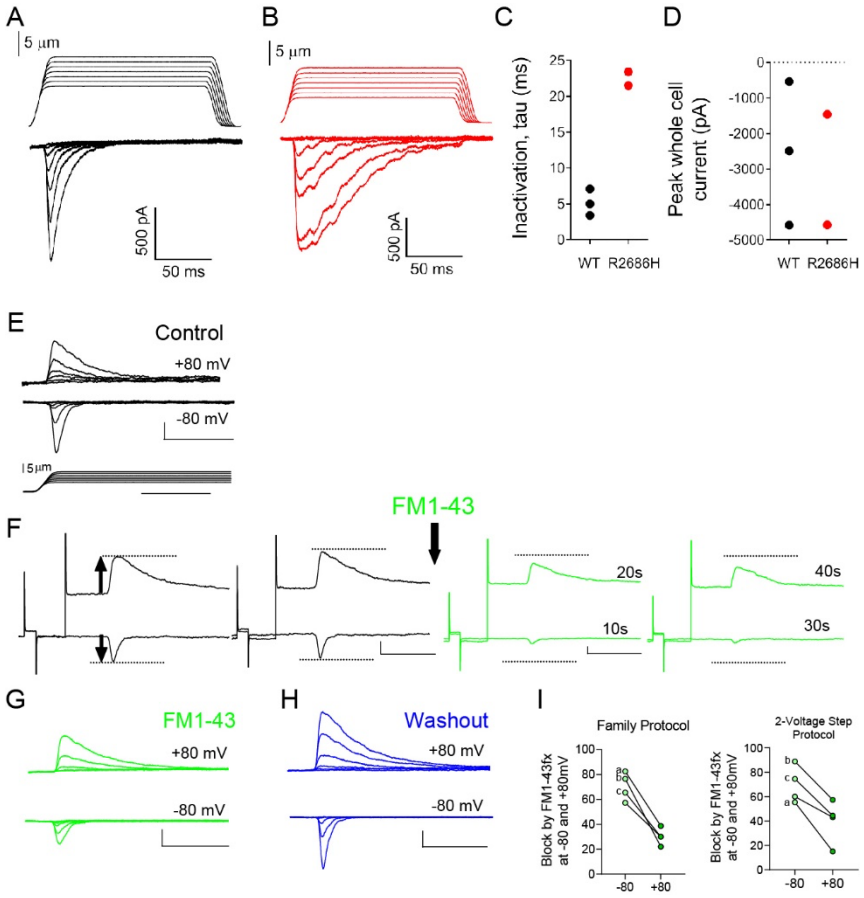


**Figure S4: *PIEZO2-R2686H* whole-cell poke characterization, and comparison of *PIEZO2* inhibition at -80 and +80 mV using two different protocols, related to Figure 5**

(A) Stimulus-dependent mechanically activated (poke) whole cell currents from HEK P1KO cells transiently transfected with wild type human *PIEZO2* were acquired in 1 µm increments (displacement protocol shown above the current traces) from a holding potential of -80 mV.

(B) Stimulus-dependent mechanically activated whole cell currents from HEK P1KO cells transiently transfected with *PIEZO2*$^{R2686H}$ were acquired in 1 µm increments (displacement protocol shown above the current traces) from a holding potential of -80 mV.

(C) Exponential fits to the inactivating phase were determined in GraphPad Prism (tau) and plotted for wild type hPIEZO2 (black symbols) and hPIEZO2-R2686H (red symbols).
(D) Peak whole cell current amplitude observed for wild type hPIEZO2 (black symbols) and hPIEZO2-R2686H (red symbols).

(E) Stimulus dependent mechanically activated (poke) currents acquired under control conditions from HEK P1KO cells transiently transfected with wild type human *PIEZO2*. Displacements shown below. All families show currents elicited by displacement of the blunt glass probe up to 5µm above the apparent threshold stimulus.

(F) Mechanically activated currents elicited by a single poke stimulus at -80 and +80mV 10s later. Protocol was repeated after 10s. FM1-43 (10µM) was rapidly bath applied by pipette as indicated at the arrow and recordings continued every 10 sec prior to acquiring families at -80 then +80mV, still in the presence of FM1-43.

(G-H) Families of stimuli were acquired after 4.5 min washout by continuous gravity perfusion.

(I) The percent inhibition at both +80 mV and -80 mV were obtained from cells tested by application of stimulus families (G-H) or by alternating voltage steps (F) or both. The data for three single cells tested by

both protocols are labelled (a, b, c). Similar results were obtained from the two methods. Representative traces are from cell "b".

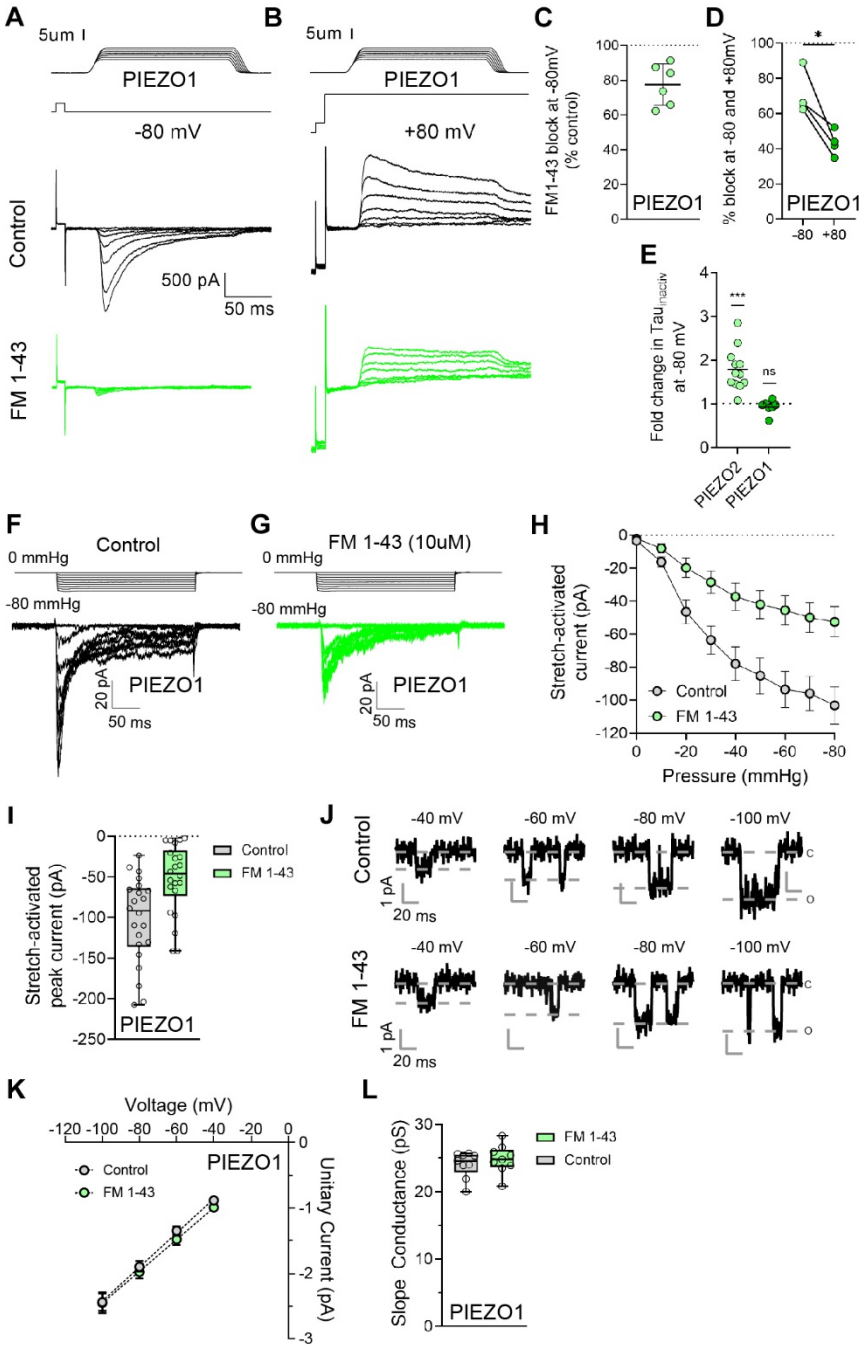


**Figure S5: FM 1-43 inhibits mechanically activated currents from PIEZO1, related to Figure 5**

(A-B) Stimulus-dependent mechanically activated (poke) whole cell currents from HEK P1KO cells transiently transfected with wild type human PIEZO1 were acquired in 1 μm increments (displacement protocol shown above the current traces) from a holding potential of either -80 mV (A) or +80 mV (B) before (Control, black traces) and during exposure to 10 μM FM1-43 (FM1-43, green traces). Currents are leak subtracted relative to levels prior to the mechanical stimulus. The scale bars for all families of currents (A-B) are shown in the control family in A.

(C) Inhibition of hPIEZO1-mediated MA currents is plotted as a percent of control for n= 6 cells.

(D) When inhibition was possible to determine at +80 mV for an individual cell (n=4), the data from an individual cell is connected. P=0.0242 (*)

(E) Tau of inactivation was slowed by FM1-43 only for hPIEZO2 (light green symbols) and not hPIEZO1 (dark green symbols). Plotted is the fold change in the inactivation tau for currents recorded at -80 mV where 1 is no change in tau.

(F) Pressure protocol (gray) and currents (black) from a representative cell-attached recording from a Neuro2a-P1KO cell expressing wild-type human Piezo1. Holding potential was -80 mV.

(G) Same as F, with 10 μM FM1-43 in the pipette solution.

(H) Mean pressure-response curves elicited by the protocol in J-K. n=22 (control), 22 (10 μM FM1-43). Data are mean ± S.E.M.

(I), Box-and-whisker plots for peak stretch-activated current at -80 mmHg, from the protocol in F-G. n=22 (control), 22 (10 μM FM1-43).

(J), Representative single-channel openings at -40 mV, -60 mV, -80 mV, and -100 mV from Neuro2a-p1ko cells expressing wild-type human Piezo1, in the absence (top) and presence (bottom) of 1 μM FM1-43 in the pipette solution. Dashed lines indicate closed (c) and open (o) states.

(K) Single-channel current as a function of voltage for the representative patches in J, with corresponding simple linear regression fits to obtain slope conductance (dashed line). Data are mean ± S.D.

(L), Box-and-whisker plots for slope conductance in control solution (n=8) and in the presence of 1 μM FM1-43 (n=8).

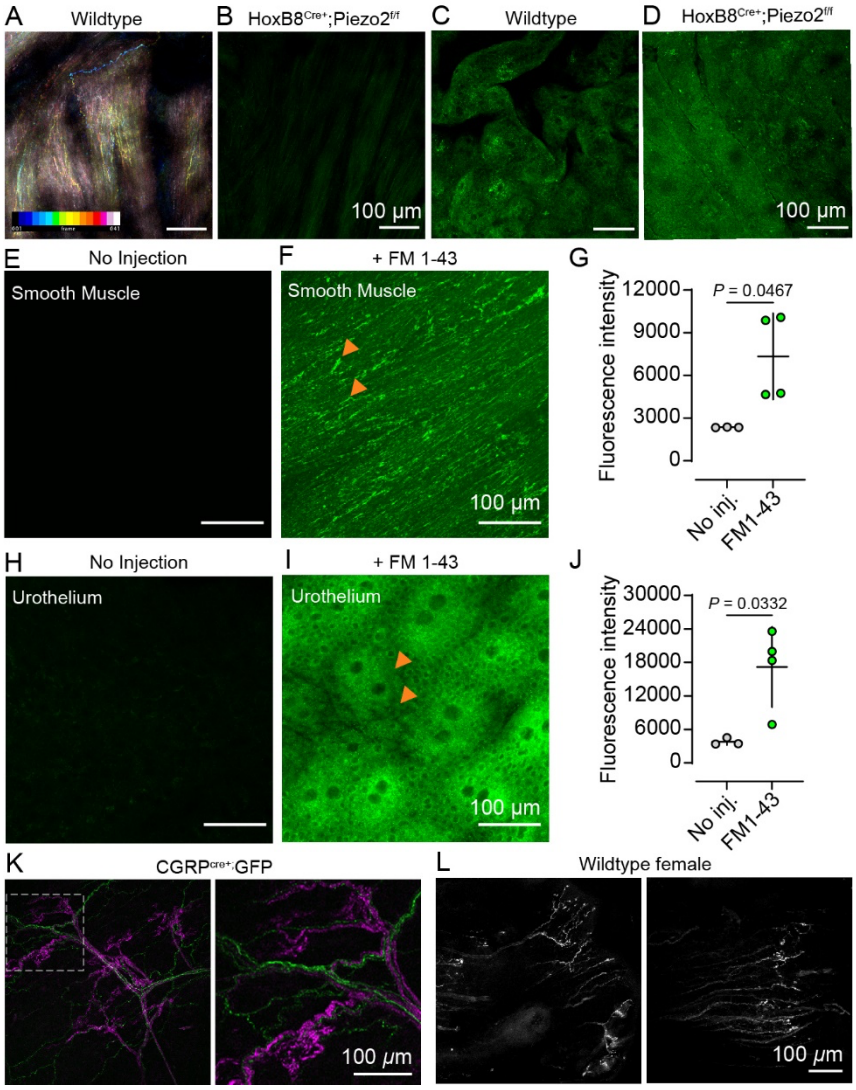


**Figure S6: Bladder smooth muscle, urothelium, and urethral labeling with FM 1-43, related to Figure 6**

(A) Representative z-stack of 41 images through the bladder of a wildtype mouse injected with FM 1-43 24 h prior. This image was taken from the muscle side. Stack was color bar coded by depth with blues indicating structures closer to the urothelium, and pink and white indicating structures within the muscle layer. A neuronal process is visible in blue.

(B) Representative z-stack through the bladder of a *HoxB8$^{Cre+}$;Piezo2$^{f/f}$* mouse injected with FM 1-43 24 h prior.

(C) Representative z-stack through the bladder, imaged from the urothelial side, in a wildtype mouse injected with FM 1-43 24 h prior.

(D) Representative z-stack through the bladder, imaged from the urothelial side, in a *HoxB8$^{Cre+}$;Piezo2$^{f/f}$* mouse injected with FM 1-43 24 h prior.

(E) Representative z-stack image of bladder smooth muscle without,

(F) and with FM 1-43 injection. Labeling observed in axons within muscle layer (arrowheads)

(G) Quantification of mean fluorescence intensity in bladder smooth muscle with and without FM 1-43 injection. N=3 ('No Injection'), N=4 ('Injection'). Individual points represent mean values from at least 12 field of view images in each bladder. Data shown with mean ± SD and analyzed using Welch's *t* test, p=0.0467 (*).

(H) Representative z-stack image of bladder urothelium without,

(I) and with FM 1-43 injection. Labeling observed in superficial cells that appear to have double nuclei (putative umbrella cells) and other urothelial cells that appear to be single nucleated, although individual cells cannot be confidently outlined (arrowheads point to one of each type).

(J) Quantification of mean fluorescence intensity in bladder urothelium with and without FM 1-43 injection. N=3 ('No Injection'), N=4 ('Injection') Individual points represent mean values from at least 10 field of view images in each bladder. Data shown with mean ± SD and analyzed using Welch's *t* test, p=0.0332 (*).

(K) Representative z-stack of pelvic urethra neurons from a $CGRP^{cre+}$;GFP mouse, i.p. injected with FM 4-64 24 h prior. GFP (green) and FM 4-64 (magenta) channels are displayed as a single merged image. Image on right is magnified from the boxed area on the left.

(L) Two examples of FM 1-43 labeled ending structures at the distal end of the female urethra.

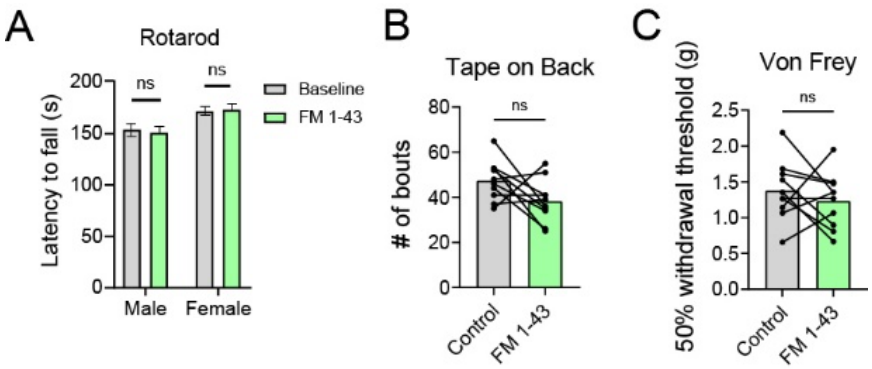


**Supplemental Figure 7: FM 1-43 does not induce mechanosensory deficits in mice, related to Figure 5**

(A) Results from rotarod test after injection with FM 1-43. N=10 mice tested, 5 males and 5 females. Bars represent mean ± S.D. Analyzed by paired two-tailed t-test, male, p=0.7489 (n.s.), female, p=0.929 (n.s.).

(B) Results from Von Frey 2 h after injection with FM 1-43. N=10 mice tested, 5 males and 5 females. Individual dots represent each animal, and means plotted as bars. Analyzed by paired two-tailed t-test, p=0.4169 (n.s.)

(C) Results from 'Tape on Back' behavioral assay 2 h after injection with FM 1-43. N=10 mice tested, 5 males and 5 females. Individual dots represent each animal, and means plotted as bars. Analyzed by paired two-tailed t-test, p=0.0930 (n.s.)